

1 **Deleterious variation mimics signatures of genomic incompatibility and adaptive**
2 **introgression**

3

4 Bernard Y. Kim¹, Christian D. Huber¹, Kirk E. Lohmueller^{1,2,3,*}

5

6 **Affiliations:**

7 ¹Department of Ecology and Evolutionary Biology, University of California, Los Angeles, CA
8 90095, USA.

9 ²Interdepartmental Program in Bioinformatics, University of California, Los Angeles, CA 90095,
10 USA.

11 ³Department of Human Genetics, David Geffen School of Medicine, University of California,
12 Los Angeles, CA 90095, USA.

13 *Corresponding author: E-mail: klohmueller@ucla.edu

14

15

16

17

18

19

20

21

22

23

24

25

26

27

28

29

30

31

32

33

34

35 **Abstract**

36 While it is appreciated that population size changes can impact patterns of deleterious
37 variation in natural populations, less attention has been paid to how population admixture affects
38 the dynamics of deleterious variation. Here we use population genetic simulations to examine
39 how admixture impacts deleterious variation under a variety of demographic scenarios,
40 dominance coefficients, and recombination rates. Our results show that gene flow between
41 populations can temporarily reduce the genetic load of smaller populations, especially if
42 deleterious mutations are recessive. Additionally, when fitness effects of new mutations are
43 recessive, between-population differences in the sites at which deleterious variants exist creates
44 heterosis in hybrid individuals. This can lead to an increase in introgressed ancestry, particularly
45 when recombination rates are low. Under certain scenarios, introgressed ancestry can increase
46 from an initial frequency of 5% to 30-75% and fix at many loci, even in the absence of beneficial
47 mutations. Further, deleterious variation and admixture can generate correlations between the
48 frequency of introgressed ancestry and recombination rate or exon density, even in the absence of
49 other types of selection. The direction of these correlations is determined by the specific
50 demography and whether mutations are additive or recessive. Therefore, it is essential that null
51 models include both demography and deleterious variation before invoking reproductive
52 incompatibilities or adaptive introgression to explain unusual patterns of genetic variation.

54 **Introduction**

55 There is tremendous interest in quantifying the effects that demographic history has had
56 on the patterns and dynamics of deleterious variation and genetic load (Kirkpatrick and Jarne
57 2000; Gazave et al. 2013; Lohmueller 2014a; Lohmueller 2014b; Henn et al. 2015; Brandvain
58 and Wright 2016; Simons and Sella 2016). Several studies have suggested that recent human
59 demography has had little impact on load (Simons et al. 2014; Do et al. 2015) while others have
60 suggested weak, but subtle differences between human populations (Casals et al. 2013; Fu et al.
61 2014; Gravel 2016; Henn et al. 2016; Pedersen et al. 2017). All of these studies have typically
62 focused on how population size changes, such as expansions and bottlenecks, have affected
63 deleterious variation. Other types of complex demography, however, have received considerably
64 less attention.

65 In particular, gene flow may be important for shaping patterns of deleterious variation.
66 Population admixture, or hybridization between closely related species, appears to be quite
67 common in nature (Payseur and Rieseberg 2016) and has a significant role in shaping human
68 genomes (Wall and Yoshihara Caldeira Brandt 2016). Gene flow alone can subtly change the

69 effects of selection on deleterious variation (Gravel 2016), but should have notable fitness
70 consequences if deleterious variation is distributed differently between admixing populations. For
71 example, Neanderthals likely had a higher genetic load than coincident human populations due to
72 the former's smaller long-term population size (Do et al. 2015; Harris and Nielsen 2016; Juric et
73 al. 2016). As a result, gene flow from Neanderthals into the ancestors of modern humans could
74 have increased the genetic load of some human populations by 0.5% (Harris and Nielsen 2016),
75 and selection should have removed deleterious Neanderthal ancestry over time. In contrast,
76 domesticated species likely have increased genetic load due to domestication bottlenecks and
77 hitchhiking with artificially selected variants (Marsden et al. 2016; Liu et al. 2017; Moyers et al.
78 2017). Then, gene flow from their wild counterparts should alleviate the genetic load of
79 domesticated species and increased levels of introgression should be observed (e.g. Wang L,
80 Beissinger TM, Lorant A, Ross-Ibarra C, Ross-Ibarra J, Hufford M, unpublished data,
81 <https://www.biorxiv.org/content/early/2017/03/07/114579>, last accessed Nov. 13, 2017).

82 If effects of gene flow can be modulated by the consequences of deleterious variation,
83 selection on deleterious variants may provide an alternative explanation for patterns of
84 introgression that are usually attributed to processes such as the evolution of reproductive
85 incompatibility or adaptive introgression. Patterns such as the depletion of introgressed ancestry
86 in regions of low recombination (Sankararaman et al. 2014) might be instead partially explained
87 by purifying selection removing deleterious variation and partially by reproductive
88 incompatibilities (Sankararaman et al. 2014; Harris and Nielsen 2016; Juric et al. 2016; Vernet et
89 al. 2016). Rampant adaptive introgression may create the opposite pattern where there is
90 increased amounts of introgressed ancestry in regions of low recombination (e.g. Pool 2015;
91 Corbett-Detig and Nielsen 2017). Alternatively, this pattern could be due to selection favoring
92 introgressed haplotypes from a larger population that carries fewer deleterious variants. The
93 general extent of these effects in nature and their magnitude given realistic parameter
94 combinations remains to be studied.

95 Another significant issue with many models incorporating deleterious variation is the
96 assumption that fitness effects are strictly additive. A considerable proportion of strongly
97 deleterious new mutations are likely to be fully recessive or partially recessive (Simmons and
98 Crow 1977; Agrawal and Whitlock 2011; Huber CD, Durvasula A, Hancock AM, Lohmueller
99 KE, unpublished data, <https://www.biorxiv.org/content/early/2017/08/31/182865>, last accessed
100 Nov. 13, 2017). In addition, if some proportion of deleterious recessive variants is private to a
101 population, admixed populations should experience heterosis since deleterious variants are more
102 likely to be found in a heterozygous state (Crow 1948). As a result, heterosis can increase

103 effective migration rates between populations (Ingvarsson and Whitlock 2000) and may play a
104 significant role in determining the fitness of highly structured populations (Whitlock et al. 2000).
105 Heterosis may also increase introgression and the probability that introgressed ancestry will
106 persist in an admixed population, even if the introgressed ancestry contains more deleterious
107 variation (Harris and Nielsen 2016). The extent to which heterosis contributes to increases in the
108 frequency of introgressed ancestry and confounds inference of adaptive introgression is also not
109 well understood.

110 The objective of this study is to develop a clearer picture of the effect of deleterious
111 variants on fitness and the dynamics of introgression in admixing populations. Further, we aim to
112 understand how inferences of selection on introgressed ancestry are impacted by deleterious
113 variation. Previous simulation and empirical work have shown that for at least some systems,
114 deleterious variation is a significant factor modulating gene flow (Harris and Nielsen 2016; Juric
115 et al. 2016; Wang et al. 2017), but few studies have investigated these questions outside of
116 demographic models specific to a species or system. Our present study fills this void by
117 presenting a series of simulations utilizing demographic models that generalize biological
118 scenarios of interest. We include a realistic distribution of fitness effects for both additive and
119 recessive mutation models. In addition, we examine how the relationship between introgressed
120 ancestry and recombination rates, or functional content, is determined by the underlying
121 demography.

123 **Results**

124 *Forward simulations*

125 We used SLiM 4.2.2 (Haller and Messer 2017) to simulate admixture in the presence of
126 deleterious variation. In general, the underlying demographic model was a population split model
127 with an ancestral population size (N_a) of 10,000 diploids, where a single pulse of admixture
128 occurs at an initial proportion of 5%, in one direction and for one generation, at some time after
129 the split (**Figure 1, Table 1**). Throughout, we will refer to the subpopulation from which gene
130 flow occurs as the *source* subpopulation, and the subpopulation which receives gene flow as the
131 *recipient* subpopulation. Furthermore, we will refer to ancestry in the recipient subpopulation that
132 originated in the source subpopulation as *introgression-derived ancestry*. We tracked the
133 frequency of introgression-derived ancestry in simulations by placing marker mutations in one
134 subpopulation, and use p_I to denote the estimated total proportion of ancestry in the recipient
135 subpopulation that is introgression-derived. The sizes of the subpopulations were varied as
136 described in the forthcoming sections and in **Figure 1** and **Table 1**.

137 Unless specified otherwise, we simulated approximately 5 Mb of sequence, with
138 randomly generated genic structure (see Methods). The mutation rate (μ) was set at a constant rate
139 of 1.5×10^{-8} per bp per generation. All simulated mutations were either neutral or deleterious, and
140 only nonsynonymous mutations had nonzero selection coefficients. Deleterious mutations had
141 selection coefficients (s) were all drawn from the same distribution of fitness effects (Kim et al.
142 2017). In other words, the selection coefficients did not depend on the population in which
143 mutations occurred. No positively selected mutations were simulated in any of our models. We
144 simulated additive ($h=0.5$) and recessive ($h=0.0$) mutations separately. Additive fitness effects
145 were computed by multiplicatively calculating fitness at each locus. Recessive fitness effects
146 were computed additively, but only at homozygous loci. All fitness effects were computed
147 multiplicatively across loci. To assess the effect of recombination rate, we also varied the per-
148 base pair per chromosome recombination rate, r , between sets of simulations ($r \in \{10^{-6}, 10^{-7}, 10^{-8}, 10^{-9}\}$). See **Methods** for additional details on the simulations and calculation of fitness.

150 In each simulation, we recorded the fitness of each subpopulation, the proportion of
151 ancestry that is introgression-derived, and other measures of genetic load (**Figures S1-S3**) at
152 different time points. Differences in subpopulation fitness are presented as (w_R/w_S) , which
153 represents the relative differences in load between the recipient and source subpopulation.
154 Subpopulation fitnesses are presented separately in **Figure S1**.

155
156 *The effect of admixture on deleterious variation*

157 Our first step was to look at only the effects of gene flow on deleterious variation when
158 the two subpopulations had identical sizes. Given that the populations were of identical size, they
159 both should contain similar amounts of deleterious variation and similar genetic loads. Here, we
160 simulated under a population split model with a size of 10,000 diploids in the ancestral and both
161 divergent subpopulations (Model 0, **Figure 1**), where 20,000 ($2N_A$) generations after the
162 population split a single pulse of admixture occurred.

163 Under the additive fitness model, the fitness of the recipient subpopulation does not
164 change due to gene flow (Model 0, **Figure 2**). At the time point of admixture, the two
165 subpopulations have similar fitnesses due to identical population sizes ($w_S \approx w_R$, **Figures 2** and
166 **S1**), although many deleterious variants will be private to each subpopulation. In addition, gene
167 flow does not change the mean number of deleterious variants per haplotype, since any
168 introgression-derived haplotypes carry, on average, the same number of derived variants as
169 background haplotypes (**Figure S2**).

170 When deleterious mutations are recessive instead of additive, admixture is predicted to
171 generate heterosis in hybrid individuals, particularly when some proportion of segregating
172 variants is private to each subpopulation (Crow 1948; Whitlock et al. 2000; Harris and Nielsen
173 2016). Indeed, 20,000 generations after the population split, many of the deleterious variants in
174 our simulations should be private to one subpopulation (**Figure S4**). At the time of gene flow,
175 both subpopulations have declined in fitness to a similar degree ($w_R \approx w_S$, Model 0, **Figure 2**).
176 After admixture, homozygosity in the recipient population is immediately decreased (**Figure S3**),
177 with a corresponding increase in the fitness of the recipient population (**Figures 2 and S1**).
178 Importantly, the number of derived deleterious variants per haplotype in the recipient
179 subpopulation is unaffected by gene flow (**Figure S2**). After the initial increase in fitness due to
180 admixture, the decline in fitness following admixture is slow, such that fitness will be greater than
181 the pre-admixture value for many generations following admixture (Model 0, $h=0$, **Figure S1**).
182 Notably, the fitness increase conferred by heterosis is the most pronounced ($\approx 2.5\%$ increase) and
183 lasts the longest ($>10,000$ generations after admixture) in simulations with low amounts of
184 recombination ($r=10^{-9}$). This occurs for two reasons. First, fitness declines more quickly when
185 recombination rates are low (Muller 1964), resulting in stronger selection against non-admixed
186 individuals. Second, introgression-derived haplotypes remain intact, maximizing the heterotic
187 advantage of admixed individuals.

188 The effect of selection on deleterious variation also influences the fraction of ancestry
189 that is introgressed in the recipient population. Considering that immediately following
190 admixture, 5% of the ancestry in the recipient population is introgression-derived ($p_I=5\%$), it
191 follows that in the absence of allele frequency changes due to selection the expected proportion of
192 introgression-derived ancestry should remain $E[p_I]=5\%$. Our simulations show that this is the
193 case when fitness effects are additive and both subpopulations have similar genetic loads (Model
194 0 in **Figure 3**). Therefore, selection does not favor haplotypes of a particular ancestry, and the
195 long-term $p_I \approx 5\%$.

196 If deleterious mutations are recessive, introgression-derived ancestry increases in
197 frequency as protective haplotypes rise in frequency through heterosis ($p_I > 5\%$; Model 0, $h=0$,
198 **Figure 3**). The increase in p_I is inversely related to the recombination rate. Specifically, the
199 increase in p_I is greatest (average $p_I \sim 35\%$ at 10,000 generations after the split, **Figure 3**) for the
200 lowest recombination rate $r=10^{-9}$, (**Figures 2 and S1**). This effect is still observed even when the
201 simulated recombination rate is greater than 10^{-9} , but the magnitude of the effect is far less
202 pronounced, with increases to $p_I \approx 6-9\%$. These results also corroborate studies which showed that
203 heterosis can increase effective migration rates (Ingvarsson and Whitlock 2000) or enhance the

204 introgression of linked deleterious variants (Harris and Nielsen 2016). However, our results
205 additionally show that heterosis should be greater when recombination rates are low.

206

207 *Short-term bottlenecks have little influence on the dynamics of introgression*

208 Next, we investigated how short-term bottlenecks might affect fitness and patterns of
209 introgression by adding a short bottleneck into one subpopulation of the split model (Model 1,
210 **Figure 1**). Specifically, we added a bottleneck of size 1,000 diploids, or a 10-fold reduction in
211 population size, in the recipient subpopulation for the 50 generations immediately preceding the
212 admixture event. All population sizes remained at 10,000 diploids otherwise.

213 In this model, the additive genetic load was insensitive to the short bottleneck (Model 1,
214 **Figures 2 and S1**). Although some proportion of the deleterious variants is lost in the bottleneck,
215 the average number of deleterious variants per haplotype is unchanged (Lohmueller 2014b;
216 Simons et al. 2014; Simons and Sella 2016), and the additive load in each population is the same
217 ($w_S \approx w_R$, **Figures 2 and S1**). Therefore, gene flow has no effect on the additive load or the
218 number of deleterious variants per haplotype (**Figure S2**) in the recipient population, and there is
219 no selection on introgressed ancestry in this model.

220 We found broadly similar patterns when deleterious mutations were recessive, with some
221 important differences. Our simulations show that the bottleneck causes an additional ~2% decline
222 in the recipient population's mean fitness prior to admixture (Model 1, **Figure S1**) due to a small
223 increase in homozygosity (**Figure S3**). However, the average number of deleterious variants per
224 haplotype is unaffected by any selection against the increased proportion of homozygotes (Model
225 1, **Figure S2**). Fitness increases quickly after admixture, but consistently remains slightly less
226 than the model without a bottleneck, suggesting that any change in load due to an increased
227 number of homozygous sites is mostly cancelled out by the increased heterozygosity that results
228 from admixture (**Figure S3**). The magnitude of the fitness increase from admixture is again
229 inversely related to the recombination rate, in a manner similar to that in the model without a
230 bottleneck (Model 0).

231 The frequency of introgression-derived ancestry was largely unaffected by the short
232 bottleneck. When fitness effects were additive, the average frequency of introgressed ancestry
233 remained at the initial admixture proportion of $p_I = 5\%$, 10,000 generations after the admixture
234 event (Model 1, **Figure 3**). When fitness effects were recessive, introgression-derived ancestry
235 increased in frequency by carrying protective alleles, similar to the simulations with identical
236 subpopulation size. The same inverse relationship to the recombination rate was also observed. In
237 the case of recessive mutations, the long-term frequency of introgression-derived ancestry (e.g. p_I

238 $\approx 33\%$ for $r=10^{-9}$, Model 1 in **Figure 3**) was similar but slightly lower than the model without a
239 bottleneck (e.g. $p_I \approx 35\%$ for $r=10^{-9}$, Model 0 in **Figure 3**).

240

241 *Long-term population contractions greatly influence the dynamics of introgression*

242 At equilibrium, smaller populations will have a greater reductions of fitness due to
243 deleterious variation than larger populations (Kimura et al. 1963). Therefore, a long-term
244 reduction in population size should have different implications for fitness and the fate of
245 introgression-derived ancestry than the short bottleneck described above.

246 To investigate the effect of long-term differences in population size and subsequent gene
247 flow on patterns of deleterious alleles, we simulated a split model with the addition of a long-term
248 reduction in population size. Immediately following the split, the size of one subpopulation was
249 reduced 10-fold to 1,000 diploids (Models 2 and 3, **Figure 1**). After 20,000 additional
250 generations, gene flow occurred in a single generation at an admixture proportion of 5%. In
251 Model 2, the direction of admixture is from the small into the large population, and in Model 3
252 the direction of admixture is from the large into the small population.

253 As a consequence of long-term differences in population size, the additive fitness of the
254 small subpopulation is 7-10% less than that of the large subpopulation (Models 2 and 3 in
255 **Figures 2** and **S1**) at the time of admixture. In the additive fitness model, gene flow from the
256 small to the large subpopulation (Model 2) resulted in a small fitness decrease ($<1\%$) in the
257 recipient subpopulation's fitness, but had little effect on the average number of derived
258 deleterious variants per haplotype (**Figure S2**). Gene flow from the large to the small
259 subpopulation (Model 3) resulted in small increases ($<1\%$) in fitness in the recipient
260 subpopulation's fitness, except ($\sim 5\%$ increase) when recombination was low (**Figure S1**). In this
261 case, selection for less deleterious haplotypes resulted in an overall decrease of the average
262 number of deleterious variants per haplotype, but because the recipient population remained at a
263 small size after admixture, load continued to accumulate afterward at the same rate (**Figures 2**
264 **and S1**).

265 When deleterious mutations were recessive, the effect of admixture on the recipient
266 population's fitness was determined both by differences in genetic load between populations and
267 heterosis from admixture. Immediately prior to admixture, the recipient population's fitness was
268 approximately 10-30% greater (in Model 2) or less (in Model 3) than the fitness of the source
269 subpopulation (**Figures 2** and **S1**) due to long-term differences in population size. Gene flow
270 from the small to the large population (Model 2) only increased the recipient subpopulation's
271 fitness by 1-2% ($h=0$, **Figure S1**), and thus did not drastically affect the trajectory of w_R/w_S

272 (Figure 2). However, gene flow from the large to the small population (Model 3) drastically and
273 immediately increased the fitness of the recipient population ($h=0$, Figures 2 and S1). Because
274 the population size of the recipient subpopulation remained small in Model 3, fitness continued to
275 decline quickly after admixture. In both models, increased fitness in the recipient population after
276 admixture is a consequence of a decrease in the mean number of homozygous deleterious sites
277 per individual due to admixture. These effects are more pronounced for Model 3 because of the
278 higher number of homozygous sites per individual in the large subpopulation (on average about
279 110; Figure S3) compared to the small subpopulation (on average about 50-60; Figure S3). In
280 other words, more private recessive deleterious variants are masked by introgressing haplotypes
281 in Model 3, despite the fact that introgressing haplotypes carry a slightly larger number of
282 deleterious variants. Importantly, gene flow had little effect on the mean number of deleterious
283 variants per haplotype (Figure S2). Again, our simulations show that the fitness changes from
284 admixture should be largest when recombination rates are low.

285 Due to these differences in fitness between the small and large subpopulations, the
286 frequency of introgression-derived ancestry in the recipient population changed noticeably for
287 both the additive and recessive models (Models 2 and 3 in Figure 3). When fitness effects were
288 additive, these changes were directly linked to selection on introgressed variation. If introgressed
289 haplotypes carried a larger deleterious burden (i.e. came from the smaller population as in Model
290 2), introgressed ancestry linked to deleterious alleles was removed by selection (long-term $p_I \approx 0$ -
291 4%). On the other hand, if introgressed haplotypes had a smaller deleterious burden (i.e. came
292 from the larger population as in Model 3), linked introgression-derived ancestry increased in
293 frequency due to selection for haplotypes with fewer deleterious variants (long-term $p_I \approx 6$ -38%).
294 Again, we observe that the magnitude of this effect is inversely related to the recombination rate.
295 Specifically, the proportion of introgression-derived ancestry decreased or increased at the
296 greatest magnitude in simulations with low recombination, and the least in simulations with a
297 high recombination rate (Models 2 and 3 in Figure 3).

298 When fitness effects were recessive, the frequency of introgression-derived ancestry in
299 the recipient subpopulation were determined by heterosis and differences in genetic load between
300 subpopulations. Gene flow from the large to the small subpopulation (Model 3) resulted in slight
301 ($p_I = 7\%$, $r = 10^{-6}$) to drastic increases ($p_I = 51\%$, $r = 10^{-9}$) in the average proportion of introgression-
302 derived ancestry (Model 3, Figure 3). However, admixture from the small to the large (Model 2)
303 population resulted in smaller ($p_I \approx 6$ -17%) proportions of introgression-derived ancestry (Model
304 2, Figure 3). Additionally, the increase in frequency from selection on recessive variation
305 opposes the effect of selection on additive variation. In the case of Model 3, heterosis and

306 differences in load drive the frequency of introgression-derived ancestry in the same direction,
307 but in the case of Model 2, these factors work in opposite directions. The rate of change of the
308 proportion of introgression-derived ancestry was greatest in simulations with low recombination
309 rates ($r=10^{-9}$).

310

311 *Long-term population contractions with subsequent population recovery greatly influence the*
312 *dynamics of introgression*

313 To investigate what occurs when differences in genetic load exist between two
314 subpopulations, but where the strength of selection is increased in the recipient population post-
315 admixture, we simulated another split model where the recipient subpopulation is subjected to a
316 long-term bottleneck but recovers to its original size (Model 4, **Figure 1**). Specifically, the model
317 we simulated was a split model where the recipient subpopulation is reduced to 1,000 diploids
318 immediately after the population split and for 20,000 generations afterwards. At that time point,
319 gene flow occurred in a single generation at an admixture proportion of 5%. Immediately
320 following the admixture event, the recipient subpopulation was restored to its original size
321 (10,000 diploids).

322 Like the model where the recipient subpopulation size remained small after the split
323 (Model 3), immediately prior to admixture, the recipient population's fitness was approximately
324 7-10% less than the fitness of the source population when mutations were additive and 10-30%
325 less than the fitness of the source subpopulation when mutations were recessive (**Figures 2** and
326 **S1**). When mutations were additive, admixture and population recovery result in a gradual
327 increase in the recipient subpopulation's fitness ($h=0.5$, **Figures 2** and **S1**). When mutations were
328 recessive, admixture rapidly increases the fitness of the recipient subpopulation to at least 90%
329 and up to 95% of its pre-bottleneck fitness, then continues to recover slowly thereafter ($h=0.0$,
330 **Figures 2** and **S1**). In both cases, gene flow results in substantial decreases in the number of
331 deleterious variants per haplotype (**Figure S2**) as well as the number of homozygous deleterious
332 sites per individual (**Figure S3**). The quickest increase in fitness is again observed in the
333 simulations with the lowest recombination rate ($r=10^{-9}$; **Figures 2** and **S1**).

334 Large changes in subpopulation fitness are tied to the largest changes in the frequency of
335 introgression-derived ancestry in the recipient subpopulation (Model 4 in **Figure 3**). When
336 mutations are additive, the fraction of introgression-derived ancestry quickly increases from an
337 initial $p_I=5\%$ to $p_I\approx 7-68\%$, with higher long-term fractions of introgression-derived ancestry
338 occurring at lower recombination rates. When mutations are recessive, the fraction of
339 introgression-derived ancestry has increases to $p_I\approx 10-74\%$. Thus, the population expansion after

340 the bottleneck drives a rapid increase in the frequency of introgressed ancestry in the recipient
341 population.

342

343 *Increasing population split times enhances the effect of heterosis*

344 In models where fitness effects are recessive, heterosis, although modulated by
345 subpopulation differences in genetic load, determines the fitness effects of admixture and the
346 direction of selection on introgression-derived ancestry. However, in these simulations, we have
347 fixed the split time before admixture at $2N$ generations, a substantially long time for private
348 deleterious variation to accumulate within each subpopulation. To further examine the
349 relationship between split time and selection on introgression-derived ancestry, we simulated split
350 models while varying the split time before gene flow. Specifically, we simulated gene flow
351 between two populations of equal size; one where the recipient population experienced a brief
352 bottleneck of 1,000 diploids for the 50 generations immediately before the admixture event; and
353 one where the recipient population's size was reduced to 1,000 diploids immediately after the
354 split until a single pulse of admixture at 5%, where it then recovered to the original size of 10,000
355 diploids. These models are analogous to Models 0 and 4 (**Figure 1**), respectively, the only
356 difference being the split time before admixture. The recombination rate was set to $r=10^{-9}$ in these
357 simulations.

358 **Figure 4** depicts the long-term proportion of introgressed ancestry, p_I , 10,000 generations
359 after the single pulse of admixture for these three models varying the amount of time between the
360 split and admixture (t_s). First, we found that across our range of simulated t_s , p_I always increases
361 monotonically with t_s , regardless of the underlying demography (**Figure 4**). This can be attributed
362 to the fact that longer split times result in more deleterious variation being unique to each
363 population (**Figure S4**), enhancing heterosis after admixture. Second, we found as a bottleneck
364 increases in duration, differences in genetic load become a significant contributor to long-term p_I .
365 At a split time and thus bottleneck time of 20,000 generations, the effects of heterosis and the
366 bottleneck increase long-term p_I nearly 2-fold relative to heterosis alone (compare Model 0 to
367 Model 4 in **Figure 4**).

368

369 *A realistic map of chromosomal structure and recombination rates*

370 Thus far we have shown how selection on deleterious variation can affect the dynamics
371 of introgression-derived ancestry when the recombination rate was set to a single value in each
372 set of our simulations. The correlation between introgression-derived ancestry and genomic
373 features such as local recombination rates or exon density are often considered potential evidence

374 for selection against introgression-derived ancestry due to genomic incompatibility or
375 maladaptive alleles (Brandvain et al. 2014; Sankararaman et al. 2014; Pool 2015; Aeschbacher et
376 al. 2017; Corbett-Detig and Nielsen 2017) or adaptive introgression (Corbett-Detig and Nielsen
377 2017). Selection on deleterious variation is one possible confounder of these patterns (Harris and
378 Nielsen 2016; Juric et al. 2016; Wang et al. 2017).

379 To investigate how the correlation of introgression-derived ancestry with genomic
380 features is influenced by deleterious variation under different demographic models, we simulated
381 a 100 Mb segment of human chromosome 1, using realistic exon definitions and a recombination
382 map defined on a 10 kb scale (see **Methods**). Unlike the simulations we described previously, we
383 fixed the exon definitions and recombination map to be the same in all simulations. We simulated
384 under three of the split models described previously (**Figure 1**): Model 0, Model 2, and Model 4,
385 separately for recessive and additive fitness effects. Only deleterious mutations were simulated.
386 At the end of each simulation, we split the chromosome into non-overlapping 100 kb windows
387 and computed the frequency of introgression-derived ancestry, exon density, and the average
388 recombination rate in each window.

389 The average genomic landscape of introgression for 100 simulation replicates varied
390 widely across demographic models and dominance coefficients (**Figure 5** or see **Figure S5** for a
391 representative single simulation replicate). In general, simulations with recessive mutations
392 always showed a genome-wide increase in the frequency of introgressed ancestry, and
393 simulations with additive fitness were dependent upon the demographic model. In the model with
394 equal population sizes (Model 0), we observed no average change in the frequency of
395 introgression-derived ancestry when mutations were additive, but when mutations were recessive
396 we observed a large overall genome-wide increase in the frequency of introgression-derived
397 ancestry (**Figure 5**), with several regions that are at high frequency or fixed in a single simulation
398 replicate (**Figure S5**). Importantly, this increase in frequency is only due to selection on recessive
399 mutations and local variation in recombination rate, since no positively selected mutations were
400 simulated. In the model where introgressed haplotypes contained a larger deleterious burden
401 (Model 2), we observed an overall depletion of introgressed ancestry consistent with the effects
402 of purifying selection upon introgressed ancestry (**Figure 5**). However, for the model with
403 recessive mutations, the effects of heterosis were strong enough such that many genomic regions
404 showed average increases in frequency of 5-10% in our simulations. Importantly, Harris and
405 Nielsen (2016) predicted that heterosis would increase the frequency of introgressed ancestry by
406 only a few percent, but our simulations with a similar demographic model show that low
407 recombination rates can greatly enhance the increase in frequency of introgressed ancestry.

408 Finally, when we simulated the introgression of haplotypes from a population with lower genetic
409 load (Models 3 and 4), we observed drastic, genome-wide increases in the average frequency of
410 introgressed ancestry in the recipient subpopulations (**Figure 5**) as well as many fixed loci in
411 individual simulations (**Figure S5**), regardless of whether fitness effects of mutations were
412 additive or recessive. For example, local regions of the simulated chromosome showed an
413 increase in introgressed ancestry from an initial frequency of 5% up to 70-80% frequency. This is
414 the type of signature that would be unlikely to be generated under neutral demographic models
415 and could be attributed to adaptive introgression.

416 It is also notable that the frequency of introgression-derived ancestry (p_I) in each window
417 appears to be driven by exon density, or the local concentration of sites at which deleterious
418 mutations can occur. For recessive mutations, p_I is greatly increased on the left-hand side of the
419 simulated chromosome, which tends to be more gene-rich than the right-hand side of the
420 chromosome (**Figures 5** and **S5**). For additive mutations, the pattern is not as straightforward.
421 When introgressed ancestry is depleted in the recipient population (Model 2), this depletion is
422 strongest in the left-hand side of the figure compared to the right-hand side. In Model 4, where
423 introgressed ancestry increases in the recipient population, the increase is greatest in the most
424 gene-dense part of the chromosome.

425 We show the correlations that deleterious mutations generate between genomic features
426 and the frequency of introgressed ancestry, measured in 100 kb windows, in **Table 2**. In the
427 model of equal population sizes (Model 0), the frequency of introgression-derived ancestry is not
428 significantly related to the recombination rate or exon density when fitness is additive, but is
429 positively correlated to exon density when fitness effects are recessive. When introgressed
430 ancestry comes from the population with higher load (Model 2), the frequency of introgression-
431 derived ancestry is positively correlated to the recombination rate and negatively correlated to
432 exon density when fitness is additive. When fitness effects are recessive in this model, the
433 frequency of introgressed ancestry is only positively correlated to exon density. Lastly, when
434 introgressed ancestry comes from a larger population having a lower deleterious burden than the
435 recipient population (Model 4), a negative correlation is observed between the frequency of
436 introgression-derived ancestry and recombination rate, and a positive correlation between the
437 frequency of introgression-derived ancestry and exon density. For the last model, these
438 correlations are observed for both models of additive and recessive mutations.

439
440
441

442 Discussion

443 We have shown, through simulations, that deleterious variation can greatly influence the
444 dynamics of introgression between admixing populations, in markedly different directions for
445 different demographic scenarios and modes of dominance. In addition, the recombination rate is a
446 key parameter that determines the way in which deleterious variants accumulate between
447 populations, how selection acts on admixed individuals, how selection acts at a locus with
448 admixed ancestry, and ultimately the dynamics of introgression-derived ancestry.

449 Our work further demonstrates how demography can shape patterns of deleterious
450 variation in different populations. Previous studies have examined the role of population size
451 changes (Kirkpatrick and Jarne 2000; Lohmueller et al. 2008; Simons et al. 2014; Balick et al.
452 2015; Gravel 2016) and serial founder effect models (Peischl and Excoffier 2015; Henn et al.
453 2016) on deleterious variation. Interpreting how differences in the distribution of deleterious
454 variation impact fitness has been a contentious issue (Fu et al. 2014; Lohmueller 2014b; Do et al.
455 2015; Henn et al. 2015; Simons and Sella 2016). In this study, we observed that admixture can
456 increase the fitness of the recipient population, sometimes drastically if the source population is
457 of larger long-term effective size and thus carries lower genetic load. Generally, gene flow is
458 observed to drive smaller, subtle changes in fitness. Nevertheless, the influx of new alleles can
459 result in a rearrangement of deleterious variants in an admixed population (**Figures S2 and S3**),
460 and even subtle or no changes in fitness or the number of derived alleles per individual can lead
461 to significant shifts in the frequency of introgressed ancestry (e.g. see Model 0, $h=0$, in **Figure 3**).
462 These effects can be long lasting, persisting for thousands of generations in some of our
463 simulations (**Figures 2, 3, S1**). If gene flow or hybridization is a significant feature of a study
464 population, studies concerning load should consider the fitness consequences of admixture as
465 well as population size changes.

466 That dynamics of introgression-derived ancestry can thus be driven by deleterious
467 variation also is particularly relevant for the study of gene flow between populations or species.
468 Patterns of introgression between hybridizing species are often asymmetric, vary across the
469 genome, and can be driven by demography at expansion fronts (Currat et al. 2008), dispersal
470 processes (Amorim et al. 2017), or by natural selection. However, when natural selection is
471 implicated as driving changes in introgression-derived ancestry, processes such as genomic
472 incompatibility or adaptive introgression are usually invoked to explain variation in introgression
473 across the genome. We have shown that standing deleterious variation, rather than differences in
474 selection on alleles transplanted onto a new genomic background or new environment, has the
475 potential to explain some of these patterns.

476 To the best of our knowledge, only a few studies have considered the contribution of
477 selection on deleterious variation to observed patterns of introgression (Ingvarsson and Whitlock
478 2000; Gravel 2016), and mostly in specific systems (Harris and Nielsen 2016; Juric et al. 2016;
479 Wang et al. 2017; Schumer M, Xu C, Powell D, Durvasula A, Skov L, Holland C, Sankararaman
480 S, Andolfatto P, Rosenthal G, Przeworski M, unpublished data,
481 <https://www.biorxiv.org/content/early/2017/11/01/212407>, accessed Nov. 11, 2017). It is possible
482 that deleterious variation may play a similar role in other species, in particular those that have
483 experienced reductions in population size or range expansions associated with human
484 demography. For example, work by Pool (2015) and Corbett-Detig and Nielsen (2017) on
485 mapping the introgression of African ancestry into North American populations of *Drosophila*
486 *melanogaster* show that the frequency of introgressed African ancestry is negatively correlated
487 with the recombination rate. This is particularly notable because the opposite relationship is
488 observed for Neanderthal ancestry in humans (Sankararaman et al. 2014) and in hybridizing
489 populations of swordtail fish (Schumer M, Xu C, Powell D, Durvasula A, Skov L, Holland C,
490 Sankararaman S, Andolfatto P, Rosenthal G, Przeworski M, unpublished data,
491 <https://www.biorxiv.org/content/early/2017/11/01/212407>, accessed Nov. 11, 2017), where
492 regions of the genome with high recombination rate are enriched for introgressed ancestry. Our
493 simulations show that selection on deleterious variants can plausibly explain these opposing
494 patterns in different species.

495 Originating in Africa, *D. melanogaster* has serially colonized the world in association
496 with humans (Stephan and Li 2006; Duchon et al. 2013), including parts of North America
497 approximately a hundred years ago (Keller 2007). If derived populations of *D. melanogaster* have
498 accumulated differences in deleterious variation due to bottlenecks or increased drift at the
499 expansion front (Peischl and Excoffier 2015; Henn et al. 2016), selection in North American
500 populations may favor introgressed African ancestry simply because this ancestry came from a
501 population with a larger long-term effective size, thus carrying fewer deleterious variants. If
502 recessive deleterious variation also creates heterosis in admixed individuals of North American
503 populations of *D. melanogaster*, the effects of heterosis and population size will be synergistic,
504 further enhancing introgression in genomic regions of low recombination.

505 Importantly, we do not claim that selection on standing deleterious variation explains all
506 the patterns of introgression in *D. melanogaster* or any other species, but rather that it is a
507 plausible alternative explanation that is important to consider when testing hypotheses about the
508 nature of selection on gene flow. In swordtail fish, recombination rates are positively correlated
509 with the frequency of introgressed ancestry even when the source population has a smaller

510 effective population size than the recipient population (Schumer M, Xu C, Powell D, Durvasula
511 A, Skov L, Holland C, Sankararaman S, Andolfatto P, Rosenthal G, Przeworski M, unpublished
512 data, <https://www.biorxiv.org/content/early/2017/11/01/212407>, accessed Nov. 11, 2017). This
513 pattern is not explained by models that only include deleterious variation.

514 Because selection on additive and recessive variation can act in complementary or
515 opposing directions, our study also highlights the fundamental importance of understanding the
516 distribution of selection coefficients and the relationship to dominance coefficients in natural
517 populations (the *h-s* relationship). In this study, we simulated additive and recessive mutations
518 separately, using the same distribution of fitness effects, so that we could demonstrate the effect
519 of only changing the dominance coefficient. However, strongly deleterious new mutations are
520 more likely to be partially or fully recessive (Simmons and Crow 1977; Agrawal and Whitlock
521 2011; Huber CD, Durvasula A, Hancock AM, Lohmueller KE, unpublished data,
522 <https://www.biorxiv.org/content/early/2017/08/31/182865>, last accessed Nov. 13, 2017) and so
523 new mutations are likely to have varying degrees of recessivity.

524 The underlying demographic model will determine how these additive and recessive new
525 mutations should interact after gene flow. For example, the introgression of deleterious
526 haplotypes should be assisted by recessive deleterious mutations but impeded by additive ones,
527 leading to uncertainty about the overall contribution of the effects of deleterious variation in
528 certain scenarios, such as Neanderthal to human admixture (Harris and Nielsen 2016). In other
529 scenarios, selection on additive and recessive variants should operate in the same direction. There
530 is evidence for this type of introgression of wild teosinte into maize (Wang et al. 2017), but it is
531 difficult to disentangle the effects of selection on additive versus recessive variation.

532 Our simulations reveal that the recombination rate also influences the dynamics of
533 introgressed ancestry in the presence of deleterious variation. Models of Hill-Robertson
534 interference (Hill and Robertson 1966; Keightley and Otto 2006) predict that deleterious
535 mutations will not be removed as effectively in regions of the genome with low recombination
536 rates because they may be linked to the non-deleterious alleles at other sites. We observed the
537 opposite effect in our simulated admixed populations. Specifically, in our simulations, the fitness
538 in the admixed population increased the most for the lowest recombination rates, suggesting that
539 deleterious mutations were most effectively eliminated when recombination rates were the
540 lowest. To understand this effect, it is important to realize that selection for a haplotype will be
541 most effective when all alleles on a haplotype have fitness effects in the same direction. For
542 example, if introgression-derived ancestry carries fewer deleterious variants than the other
543 haplotypes in the recipient population, selection will act to increase the frequency of the

544 protective alleles contained within the introgressed ancestry. This applies directly to our
545 simulations of admixture since immediately following an admixture event, all the protective or
546 deleterious variants are found on the same haplotype. Higher rates of recombination will result in
547 the selected variants being shuffled onto different haplotypes, decreasing the efficacy of selection.

548 An important objective of genomic studies of hybridization is to identify loci that are
549 adaptively introgressed and to ascertain the overall importance of introgression to adaptive
550 evolution (Racimo et al. 2015). Genomic regions that contain introgressed haplotypes at high
551 frequency are considered likely candidates for adaptive introgression (Huerta-Sánchez et al. 2014;
552 Gittelman et al. 2016; Racimo et al. 2017; Richards and Martin 2017), but we have shown that
553 deleterious variation can generate similar patterns, even in the absence of new beneficial
554 mutations and local adaptation. Model-based statistical approaches that compare summary
555 statistics computed for a particular window of the genome to a simulated null distribution that
556 only accounts for demography may thus be misled by deleterious variation. Again, it may be
557 difficult to differentiate heterosis due to the masking of deleterious recessive alleles from
558 heterozygote advantage at introgressed loci, despite the fact that these are two very different
559 evolutionary processes with dramatically different biological interpretations.

560 Our results argue that new null models are needed in studies seeking to identify
561 candidates of adaptive introgression. These new null models should include deleterious genetic
562 variation, as well as complex demography. In order for these models to accurately capture the
563 dynamics of deleterious variation, they should also include realistic parameters for the DFE of
564 deleterious mutations and the relationship between dominance coefficients and selection
565 coefficients. Lastly, the new null models should also include realistic models of the variation in
566 recombination rate across the genome, as recombination rate is a key determinant of the dynamics
567 of introgression (**Figure 3**). Failure to consider deleterious variation in a realistic way in studies
568 of admixing populations or hybridizing species can mislead inferences about evolutionary
569 processes acting on the genome.

570

571 **Materials and Methods**

572 *Simulation details*

573 All simulations were performed with SLiM 4.2.2 (Haller and Messer 2017). The
574 sequences from simulations with randomly generated chromosome structure were approximately
575 5 Mb in length (see below). The simulated sequences generated using features from human
576 chromosome 1 were fixed to be exactly 100 Mb in length. Every simulation contained intergenic,
577 intronic, and exonic regions, but only nonsynonymous new mutations experienced natural

578 selection. The per base pair mutation rate was constant and set to $\mu=1.5\times 10^{-8}$. Within coding
579 sequences, we set nonsynonymous and synonymous mutations to occur at a ratio of 2.31:1 (Huber
580 et al. 2017). The selection coefficients (s) of new nonsynonymous mutations were drawn from a
581 gamma-distributed DFE with shape parameter 0.186 and expected selection coefficient $E[s] = -$
582 0.01314833 (Kim et al. 2017). We chose to simulate additive ($h=0.5$) and recessive ($h=0$) fitness
583 separately, using the same DFE for s for each simulation, to allow the effects of dominance to be
584 directly compared.

585 Importantly, we chose to discard from our simulations, and therefore from calculations of
586 fitness, mutations that were fixed in the ancestral or both subpopulations. Although fixed
587 deleterious variants contribute to the overall genetic load of finite populations, they will have no
588 effect on the relative differences between admixing subpopulations and no effect on the dynamics
589 of introgression-derived ancestry. Therefore, each fitness calculation does not reflect the true
590 fitness, but rather the fitness components that are relevant during gene flow.

591 An admixture event in SLiM is handled by modifying the way the parents in each
592 generation are chosen (SLiM manual 5.2.1). For example, at an admixture proportion of 5% the
593 recipient population reproduces as follows. Five percent of the parents of the recipient population,
594 in that generation, are chosen from the source population, and 95% of the parents are chosen from
595 the recipient population.

596

597 *Simulations with randomly generated chromosomal structure*

598 Unless specified otherwise, the chromosomal structure of each simulation was randomly
599 generated by drawing exon lengths from *Lognormal*($\mu = \log(50)$, $\sigma^2 = \log(2)$), intron lengths
600 from *Lognormal*($\mu = \log(100)$, $\sigma^2 = \log(1.5)$), and the length of noncoding regions from
601 *unif*(100,5000), following the specification in the SLiM 4.2.2 manual (7.3), which is modeled
602 after the distribution of intron and exon lengths in Deutsch and Long (1999). The per-base pair
603 recombination rate (r) was fixed in each simulation, but we varied r between different sets of
604 simulations where $r \in \{10^{-6}, 10^{-7}, 10^{-8}, 10^{-9}\}$. Lastly, we simulated 200 replicates for each set of
605 simulations, of each specific h and r .

606

607 *Simulations with fixed, realistic chromosomal structure*

608 In simulations with fixed chromosomal structure (**Figure 6**), we fixed the structure to 100
609 Mb randomly chosen from human genome build GRCh37, chromosome 1 (chr1:5,005,669-
610 105,005,669). The exon ranges were defined by the GENCODE v14 annotations (Harrow et al.

611 2012) and the sex-averaged recombination map by Kong et al. (2010), averaged over a 10 kb
612 scale.

613

614 *Avoiding heterosis in the additive fitness model*

615 Computing fitness as additive at a locus but multiplicative across loci creates artificial
616 heterosis in admixed individuals. This occurs because the product of a fitness decrease will
617 reduce fitness less than the sum of a fitness decrease. As an example, assume two deleterious
618 alleles are in a single individual, each with selection coefficient s where $s < 0$. If they are found as
619 a single homozygous site, the fitness decrease is usually computed as $(1+2s)$. If they are found in
620 two heterozygous sites, the fitness would be computed as $(1+s)^2$. This second quantity is larger
621 than the first by s^2 . Because admixed individuals are more likely to carry deleterious alleles as
622 heterozygotes than non-admixed individuals, the fitness of the admixed individuals will always
623 be higher than a non-admixed individual in the above computation of fitness even when the
624 number of deleterious variants per individual is the same.

625 Because our intent with an additive fitness model was to make the fitness effect of each
626 variant independent of its genotypic state, we computed additive fitness as purely multiplicative
627 across all deleterious variants, such that an individual j carrying i variants each with selection
628 coefficient s_i has fitness w_j :

629
$$w_j = \prod_i (1 + s_i)$$

630 This computation of fitness is approximately equivalent to additive fitness. Recessive fitness
631 effects were computed in the standard manner, that is, as $1+2s_i$ when homozygous for the
632 deleterious allele and as 1 otherwise.

633

634 *Data availability*

635 All scripts necessary for reproducing the simulations we have presented are available at
636 https://github.com/LohmuellerLab/admixture_load_scripts.

637

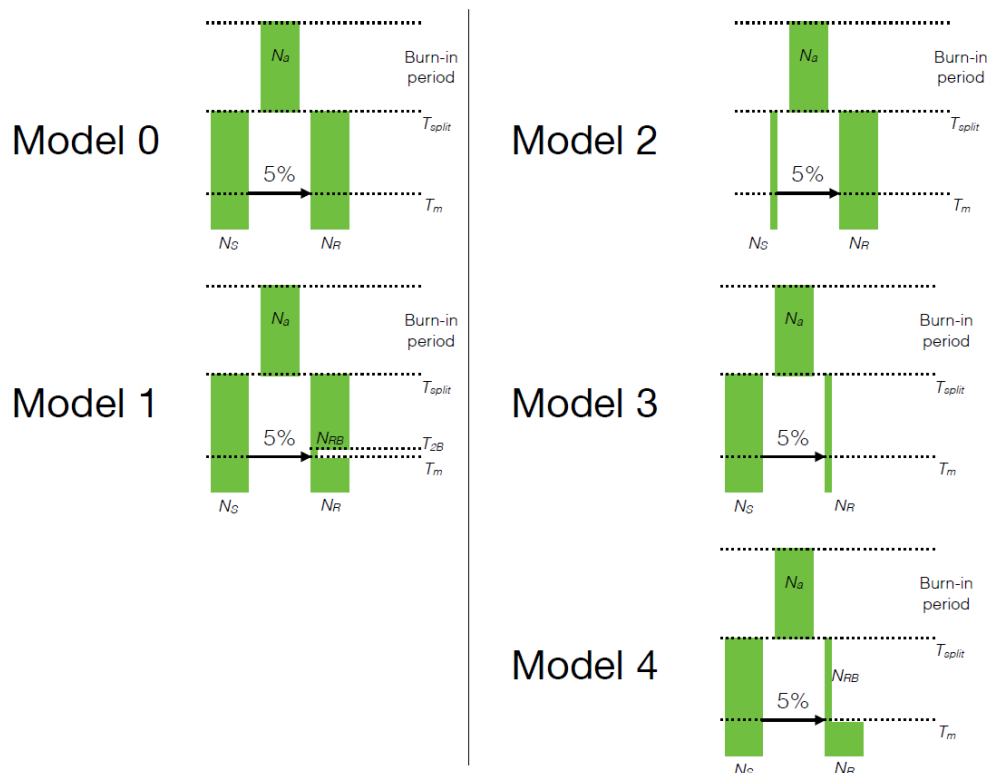
638 **Acknowledgements**

639 We thank Jacqueline Robinson, Annabel Beichman, and other members of the
640 Lohmueller Lab for helpful comments throughout the project. This work was supported by the
641 National Institutes of Health (R35 GM119856 to K.E.L.).

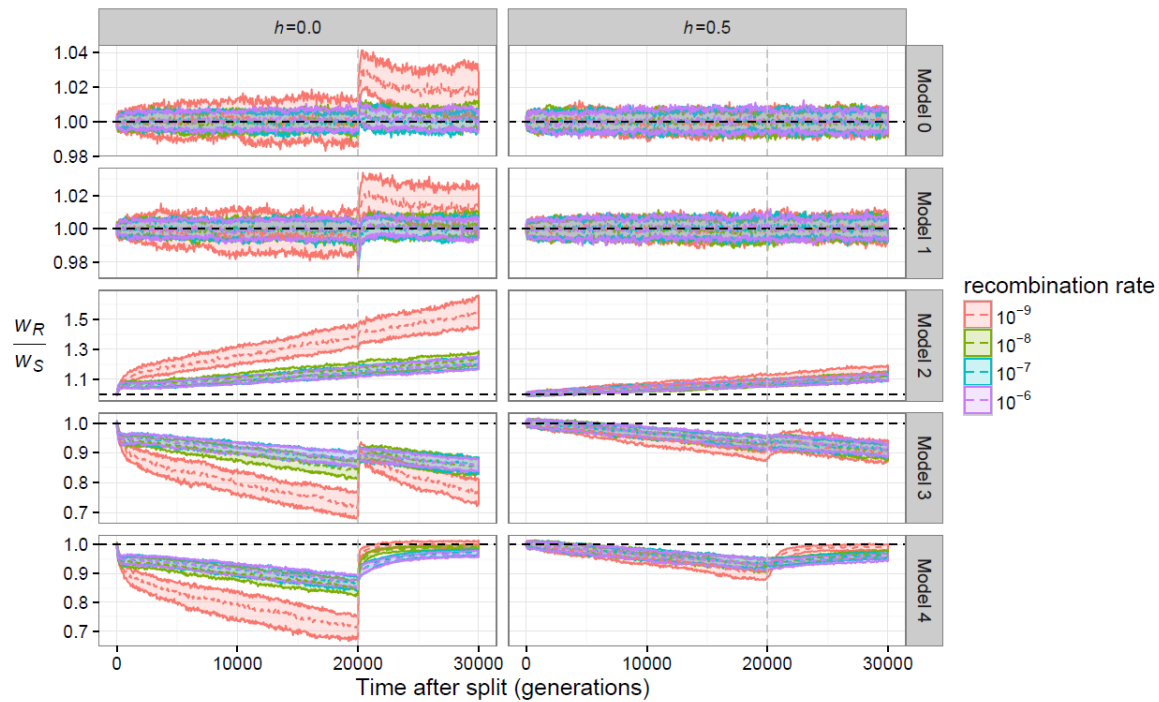
642

643

644 **Figures and Tables**

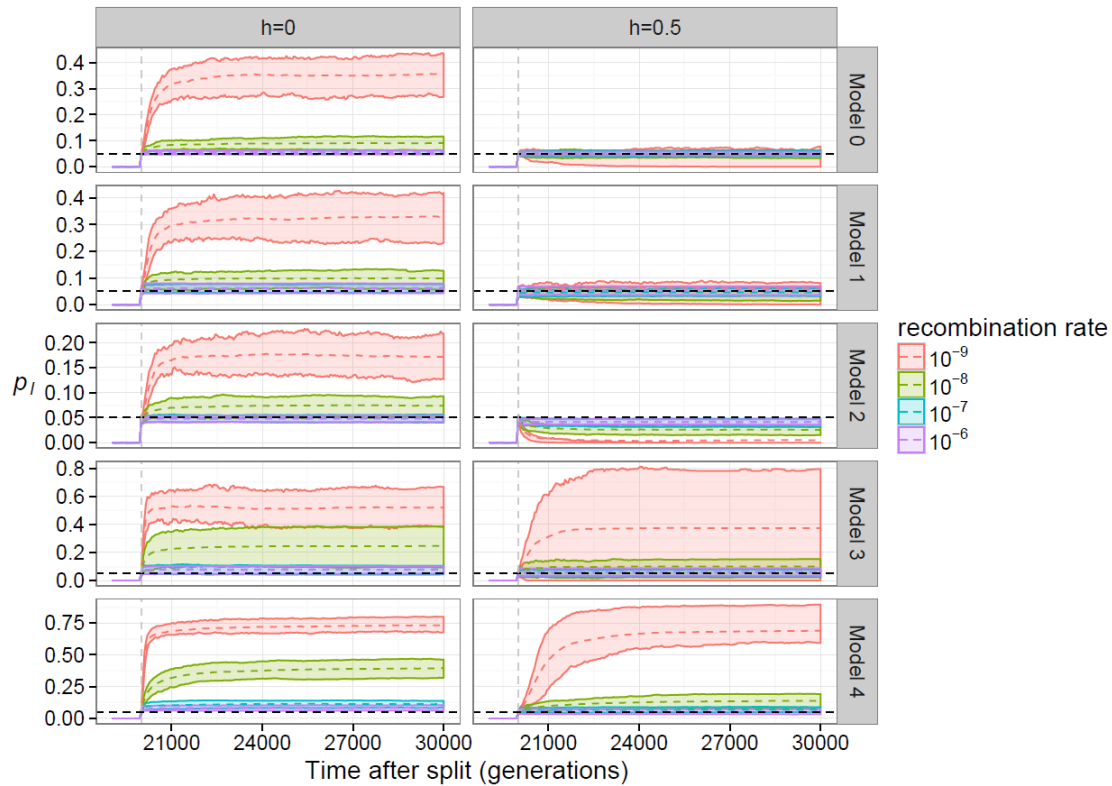


645
 646 **Figure 1.** The demographic models used for the simulations. After a burn-in period of 100,000
 647 generations, a single population diverged into two subpopulations. The demography of the
 648 subpopulations was modified in ways that changed the distribution of deleterious variation. 2,000
 649 generations after the split, a single pulse of admixture occurred such that 5% of the ancestry of
 650 the recipient population came from the donor population. Arrows in each panel denote the
 651 direction of gene flow. The simulation was run for 10,000 additional generations after admixture.
 652 Population sizes were changed as shown for each model. See **Table 1** for specific parameter
 653 values for each model.
 654



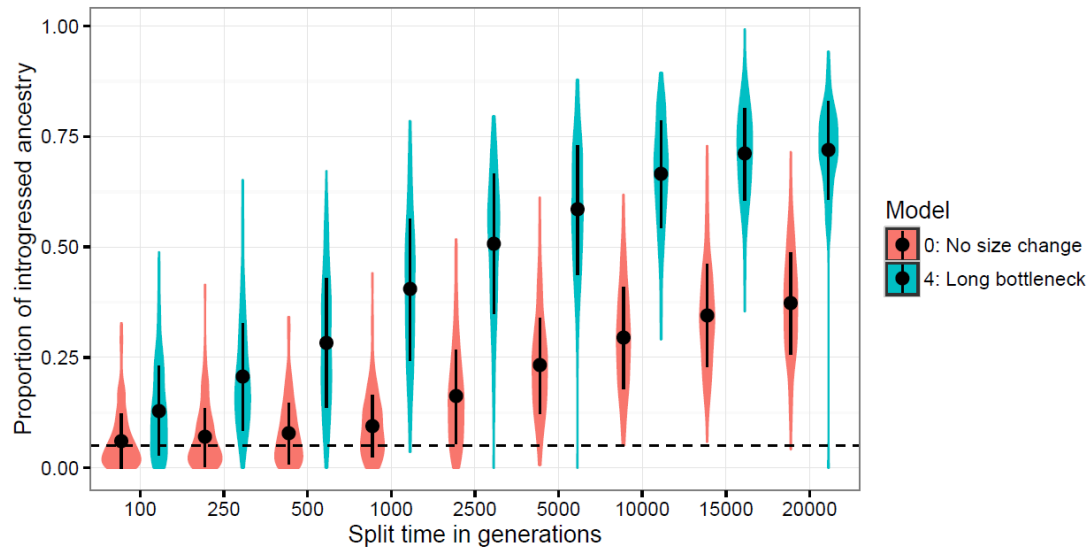
655
656 **Figure 2.** The change in mean fitness over time due to demography. Each individual plot depicts
657 the ratio of the relative mean fitness of the recipient population (w_R) to the source population (w_S)
658 for the demographic models shown in **Figure 1**. The median (dotted line) and the 25th to 75th
659 percent quantiles are shown for 200 simulation replicates. The vertical grey line depicts the time
660 of gene flow, and the horizontal black line depicts $w_R/w_S=1$. Different colors denote distinct
661 recombination rates used in the simulations. Left panel denotes recessive mutations ($h=0$) while
662 the right panel shows additive mutations ($h=0.5$).

663
664
665
666



667
668 **Figure 3.** The frequency of introgression-derived ancestry (p_I) in each model. Earlier generations
669 are not shown since $p_I=0$ prior to admixture. The mean (dotted line) and the 25th to 75th percent
670 quantiles are shown for 200 simulation replicates. The vertical red line depicts the time of gene
671 flow, and the horizontal black line depicts the initial admixture proportion of 0.05. Different
672 colors denote distinct recombination rates used in the simulations. Left panel denotes recessive
673 mutations ($h=0$) while the right panel shows additive mutations ($h=0.5$).

674
675
676
677
678
679
680



681

682

Figure 4. Population split time and population size impact the amount of introgressed ancestry

683

when mutations are recessive. The proportion of ancestry that is introgression-derived, p_I , is

684

shown for 200 simulation replicates and two demographic models (Model 0 and Model 4, refer to

685

Figure 1). The recombination rate in all simulations is $r=10^{-9}$ per base pair. Violin plots represent

686

the density while dot and whiskers represent the mean and one standard deviation to either side.

687

The horizontal black line represents the initial admixture proportion of 0.05. Note that as the split

688

time increases, p_I also increases.

689

690

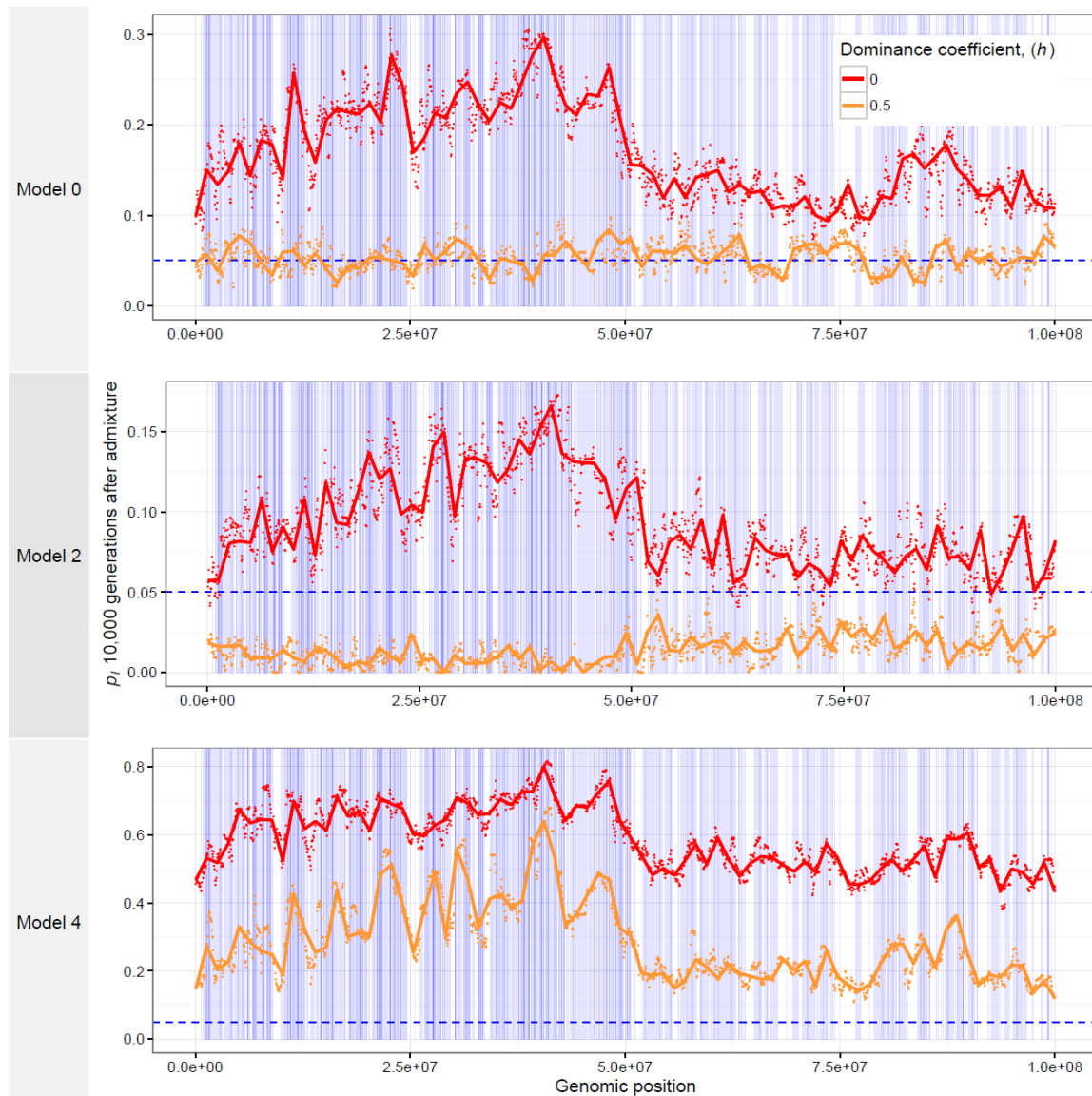
691

692

693

694

695



696

697

698

699

700

701

702

703

704

705

706

707

Figure 5. The average genomic landscape of introgression for three demographic models. The frequency of ancestry that is introgression-derived is shown for non-overlapping 100 kb windows in a simulated 100 Mb region of human chromosome 1. The model numbers refer to the models shown in **Figure 1**. Points represent a single value for each 100 kb window and lines are loess curves fitted to the data. The horizontal, blue dashed line represents the initial frequency of introgression-derived ancestry, $p_i=0.05$. Vertical blue bars represent genes in which deleterious mutations can occur. Red curves denote the results for recessive mutations while orange curves show the results for additive mutations.

708 **Table 1. Demographic parameters of the simulated models shown in Figure 1.**

Model	N_a	N_S	N_{RB}	N_R	T_m	T_{RB}	T_{split}
Model 0	10,000	10,000	--	10,000	1,000	--	3,000
Model 1	10,000	10,000	1,000	10,000	1,000	1,050	3,000
Model 2	10,000	1,000	--	10,000	1,000	--	3,000
Model 3	10,000	10,000	--	1,000	1,000	--	3,000
Model 4	10,000	10,000	1,000	10,000	1,000	--	3,000

709 NOTE.--All population sizes are in diploids and all times in generations from the present.

710 Parameters are defined as follows. N_a : ancestral population size, N_S : size of the source
 711 subpopulation, N_{RB} : size of the bottleneck in the recipient population, N_R : size of the recipient
 712 population, T_m : time of migration, T_{RB} : time at which the bottleneck in the recipient population
 713 began, T_{split} : time at which the subpopulations diverged

714

715

716

717

718 **Table 2. The correlation of recombination rate or exon density with the long-term**
 719 **frequency of introgression-derived ancestry in 100 kb windows is affected by dominance**
 720 **and demography.**

h	Genomic feature	Mean Spearman's ρ	p -value ^a
<i>Model 0</i> ^b			
0.5	recombination rate	0.003601	0.486
0.5	exon density	0.01190	0.0797
0.0	recombination rate	-0.009629	0.0859
0.0	exon density	0.09109	0
<i>Model 2</i> ^b			
0.5	recombination rate	0.01186	0.0135
0.5	exon density	-0.02972	0
0.0	recombination rate	0.0002355	0.9635
0.0	exon density	0.06164	0
<i>Model 4</i> ^b			
0.5	recombination rate	-0.06495	0
0.5	exon density	0.1743	0
0.0	recombination rate	-0.03889	0
0.0	exon density	0.1190	0

721 ^aapproximate p -values indicate the significance of H_1 : $\rho \neq 0$ and were estimated with a single
 722 sample permutation test. One hundred simulation replicates were permuted 10,000 times.

723 ^bmodel numbers reference **Figure 1**.

724

725

726 **References**

- 727 Aeschbacher S, Selby JP, Willis JH, Coop G. 2017. Population-genomic inference of the strength
728 and timing of selection against gene flow. *Proc. Natl. Acad. Sci.* 114:7061–7066.
- 729 Agrawal AF, Whitlock MC. 2011. Inferences about the distribution of dominance drawn from
730 yeast gene knockout data. *Genetics* 187:553–566.
- 731 Amorim CEG, Hofer T, Ray N, Foll M, Ruiz-Linares A, Excoffier L. 2017. Long-distance
732 dispersal suppresses introgression of local alleles during range expansions. *Heredity*
733 118:135–142.
- 734 Balick DJ, Do R, Cassa CA, Reich D, Sunyaev SR. 2015. Dominance of Deleterious Alleles
735 Controls the Response to a Population Bottleneck. *PLOS Genet.* 11:e1005436.
- 736 Brandvain Y, Kenney AM, Flagel L, Coop G, Sweigart AL. 2014. Speciation and Introgression
737 between *Mimulus nasutus* and *Mimulus guttatus*. *PLOS Genet.* 10:e1004410.
- 738 Brandvain Y, Wright SI. 2016. The Limits of Natural Selection in a Nonequilibrium World.
739 *Trends Genet.* 32:201–210.
- 740 Casals F, Hodgkinson A, Hussin J, Idaghdour Y, Bruat V, Maillard T de, Grenier J-C, Gbeha E,
741 Hamdan FF, Girard S, et al. 2013. Whole-Exome Sequencing Reveals a Rapid Change in
742 the Frequency of Rare Functional Variants in a Founding Population of Humans. *PLOS*
743 *Genet.* 9:e1003815.
- 744 Corbett-Detig R, Nielsen R. 2017. A Hidden Markov Model Approach for Simultaneously
745 Estimating Local Ancestry and Admixture Time Using Next Generation Sequence Data
746 in Samples of Arbitrary Ploidy. *PLOS Genet.* 13:e1006529.
- 747 Crow JF. 1948. Alternative Hypotheses of Hybrid Vigor. *Genetics* 33:477–487.
- 748 Currat M, Ruedi M, Petit RJ, Excoffier L. 2008. The hidden side of invasions: massive
749 introgression by local genes. *Evol. Int. J. Org. Evol.* 62:1908–1920.
- 750 Deutsch M, Long M. 1999. Intron-exon structures of eukaryotic model organisms. *Nucleic Acids*
751 *Res.* 27:3219–3228.
- 752 Do R, Balick D, Li H, Adzhubei I, Sunyaev S, Reich D. 2015. No evidence that selection has
753 been less effective at removing deleterious mutations in Europeans than in Africans. *Nat.*
754 *Genet.* 47:126–131.
- 755 Duchon P, Živković D, Hutter S, Stephan W, Laurent S. 2013. Demographic Inference Reveals
756 African and European Admixture in the North American *Drosophila melanogaster*
757 Population. *Genetics* 193:291–301.

- 758 Fu W, Gittelman RM, Bamshad MJ, Akey JM. 2014. Characteristics of Neutral and Deleterious
759 Protein-Coding Variation among Individuals and Populations. *Am. J. Hum. Genet.*
760 95:421–436.
- 761 Gazave E, Chang D, Clark AG, Keinan A. 2013. Population Growth Inflates the Per-Individual
762 Number of Deleterious Mutations and Reduces Their Mean Effect. *Genetics* 195:969–
763 978.
- 764 Gittelman RM, Schraiber JG, Vernot B, Mikacenic C, Wurfel MM, Akey JM. 2016. Archaic
765 Hominin Admixture Facilitated Adaptation to Out-of-Africa Environments. *Curr. Biol.*
766 26:3375–3382.
- 767 Gravel S. 2016. When Is Selection Effective? *Genetics* 203:451–462.
- 768 Haller BC, Messer PW. 2017. SLiM 2: Flexible, Interactive Forward Genetic Simulations. *Mol.*
769 *Biol. Evol.* 34:230–240.
- 770 Harris K, Nielsen R. 2016. The Genetic Cost of Neanderthal Introgression. *Genetics* 203:881–
771 891.
- 772 Harrow J, Frankish A, Gonzalez JM, Tapanari E, Diekhans M, Kokocinski F, Aken BL, Barrell
773 D, Zadissa A, Searle S, et al. 2012. GENCODE: The reference human genome annotation
774 for The ENCODE Project. *Genome Res.* 22:1760–1774.
- 775 Henn BM, Botigué LR, Bustamante CD, Clark AG, Gravel S. 2015. Estimating the mutation load
776 in human genomes. *Nat. Rev. Genet.* 16:333–343.
- 777 Henn BM, Botigué LR, Peischl S, Dupanloup I, Lipatov M, Maples BK, Martin AR, Musharoff
778 S, Cann H, Snyder MP, et al. 2016. Distance from sub-Saharan Africa predicts mutational
779 load in diverse human genomes. *Proc. Natl. Acad. Sci.* 113:E440–E449.
- 780 Hill WG, Robertson A. 1966. The effect of linkage on limits to artificial selection. *Genet. Res.*
781 8:269–294.
- 782 Huber CD, Kim BY, Marsden CD, Lohmueller KE. 2017. Determining the factors driving
783 selective effects of new nonsynonymous mutations. *Proc. Natl. Acad. Sci.* 114:4465–
784 4470.
- 785 Huerta-Sánchez E, Jin X, Asan, Bianba Z, Peter BM, Vinckenbosch N, Liang Y, Yi X, He M,
786 Somel M, et al. 2014. Altitude adaptation in Tibetans caused by introgression of
787 Denisovan-like DNA. *Nature* 512:194–197.
- 788 Ingvarsson PK, Whitlock MC. 2000. Heterosis increases the effective migration rate. *Proc. R.*
789 *Soc. Lond. B Biol. Sci.* 267:1321–1326.
- 790 Juric I, Aeschbacher S, Coop G. 2016. The Strength of Selection against Neanderthal
791 Introgression. *PLOS Genet.* 12:e1006340.

- 792 Keightley PD, Otto SP. 2006. Interference among deleterious mutations favours sex and
793 recombination in finite populations. *Nature* 443:89–92.
- 794 Keller A. 2007. *Drosophila melanogaster*'s history as a human commensal. *Curr. Biol.* 17:R77–
795 R81.
- 796 Kim BY, Huber CD, Lohmueller KE. 2017. Inference of the Distribution of Selection
797 Coefficients for New Nonsynonymous Mutations Using Large Samples. *Genetics*
798 206:345–361.
- 799 Kimura M, Maruyama T, Crow JF. 1963. The Mutation Load in Small Populations. *Genetics*
800 48:1303–1312.
- 801 Kirkpatrick M, Jarne P. 2000. The Effects of a Bottleneck on Inbreeding Depression and the
802 Genetic Load. *Am. Nat.* 155:154–167.
- 803 Kong A, Thorleifsson G, Gudbjartsson DF, Masson G, Sigurdsson A, Jonasdottir A, Walters GB,
804 Jonasdottir A, Gylfason A, Kristinsson KT, et al. 2010. Fine-scale recombination rate
805 differences between sexes, populations and individuals. *Nature* 467:1099–1103.
- 806 Liu Q, Zhou Y, Morrell PL, Gaut BS. 2017. Deleterious Variants in Asian Rice and the Potential
807 Cost of Domestication. *Mol. Biol. Evol.* 34:908–924.
- 808 Lohmueller KE. 2014a. The Impact of Population Demography and Selection on the Genetic
809 Architecture of Complex Traits. *PLOS Genet* 10:e1004379.
- 810 Lohmueller KE. 2014b. The distribution of deleterious genetic variation in human populations.
811 *Curr. Opin. Genet. Dev.* 29:139–146.
- 812 Lohmueller KE, Indap AR, Schmidt S, Boyko AR, Hernandez RD, Hubisz MJ, Sninsky JJ, White
813 TJ, Sunyaev SR, Nielsen R, et al. 2008. Proportionally more deleterious genetic variation
814 in European than in African populations. *Nature* 451:994–997.
- 815 Marsden CD, Vecchyo DO-D, O'Brien DP, Taylor JF, Ramirez O, Vilà C, Marques-Bonet T,
816 Schnabel RD, Wayne RK, Lohmueller KE. 2016. Bottlenecks and selective sweeps
817 during domestication have increased deleterious genetic variation in dogs. *Proc. Natl.*
818 *Acad. Sci.* 113:152–157.
- 819 Moyers BT, Morrell PL, McKay JK. 2017. Genetic costs of domestication and improvement. *J.*
820 *Hered.* esx069, <https://doi.org/10.1093/jhered/esx069>
- 821 Muller HJ. 1964. The relation of recombination to mutational advance. *Mutat. Res. Mol. Mech.*
822 *Mutagen.* 1:2–9.
- 823 Payseur BA, Rieseberg LH. 2016. A genomic perspective on hybridization and speciation. *Mol.*
824 *Ecol.* 25:2337–2360.

- 825 Pedersen C-ET, Lohmueller KE, Grarup N, Bjerregaard P, Hansen T, Siegismund HR, Moltke I,
826 Albrechtsen A. 2017. The Effect of an Extreme and Prolonged Population Bottleneck on
827 Patterns of Deleterious Variation: Insights from the Greenlandic Inuit. *Genetics* 205:787–
828 801.
- 829 Peischl S, Excoffier L. 2015. Expansion load: recessive mutations and the role of standing genetic
830 variation. *Mol. Ecol.* 24:2084–2094.
- 831 Pool JE. 2015. The Mosaic Ancestry of the *Drosophila* Genetic Reference Panel and the *D.*
832 *melanogaster* Reference Genome Reveals a Network of Epistatic Fitness Interactions.
833 *Mol. Biol. Evol.* 32:3236–3251.
- 834 Racimo F, Marnetto D, Huerta-Sánchez E. 2017. Signatures of Archaic Adaptive Introgression in
835 Present-Day Human Populations. *Mol. Biol. Evol.* 34:296–317.
- 836 Racimo F, Sankararaman S, Nielsen R, Huerta-Sánchez E. 2015. Evidence for archaic adaptive
837 introgression in humans. *Nat. Rev. Genet.* 16:359–371.
- 838 Richards EJ, Martin CH. 2017. Adaptive introgression from distant Caribbean islands contributed
839 to the diversification of a microendemic adaptive radiation of trophic specialist pupfishes.
840 *PLOS Genet.* 13:e1006919.
- 841 Sankararaman S, Mallick S, Dannemann M, Prüfer K, Kelso J, Pääbo S, Patterson N, Reich D.
842 2014. The genomic landscape of Neanderthal ancestry in present-day humans. *Nature*
843 507:354–357.
- 844 Simmons MJ, Crow JF. 1977. Mutations affecting fitness in *Drosophila* populations. *Annu. Rev.*
845 *Genet.* 11:49–78.
- 846 Simons YB, Sella G. 2016. The impact of recent population history on the deleterious mutation
847 load in humans and close evolutionary relatives. *Curr. Opin. Genet. Dev.* 41:150–158.
- 848 Simons YB, Turchin MC, Pritchard JK, Sella G. 2014. The deleterious mutation load is
849 insensitive to recent population history. *Nat. Genet.* 46:220–224.
- 850 Stephan W, Li H. 2006. The recent demographic and adaptive history of *Drosophila*
851 *melanogaster*. *Heredity* 98:65–68.
- 852 Vernot B, Tucci S, Kelso J, Schraiber JG, Wolf AB, Gittelman RM, Dannemann M, Grote S,
853 McCoy RC, Norton H, et al. 2016. Excavating Neandertal and Denisovan DNA from the
854 genomes of Melanesian individuals. *Science*:aad9416.
- 855 Wall JD, Yoshihara Caldeira Brandt D. 2016. Archaic admixture in human history. *Curr. Opin.*
856 *Genet. Dev.* 41:93–97.
- 857 Whitlock MC, Ingvarsson PK, Hatfield T. 2000. Local drift load and the heterosis of
858 interconnected populations. *Heredity* 84 (Pt 4):452–457.